Design of Piezoresistive MEMS Accelerometer with Optimized Device Dimension

A Thesis Submitted in Partial Fulfilment

of the Requirements for the Degree of

Bachelor of Technology

in

Mechanical Engineering

by

Pradosh Pritam Dash

Roll No. **111ME0292**

Under the supervision of

Prof. Subrata Kumar Panda

Department Of Mechanical Engineering

National Institute Of Technology Rourkela

Rourkela-769008

Orissa, India

May 2015

Design of Piezoresistive MEMS Accelerometer With Optimized Device Dimension

A Thesis Submitted in Partial Fulfilment

of the Requirements for the Degree of

Bachelor of Technology

in

Mechanical Engineering

by

Pradosh Pritam Dash

Roll No. **111ME0292**

Under the supervision of

Prof. Subrata Kumar Panda

Department Of Mechanical Engineering

National Institute Of Technology Rourkela

Rourkela-769008

Orissa, India

May 2015

National Institute Of Technology Rourkela

CERTIFICATE

This is to certify that the work in this thesis entitled *"Design of Piezoresistive MEMS Accelerometer with Optimized Device Dimension"* by Pradosh Pritam Dash, has been carried out under my supervision in partial fulfilment of the requirements for the degree of Bachelor of Technology in Mechanical Engineering during session 2014-2015 in the Department of Mechanical Engineering, National Institute of Technology, Rourkela.

To the best of my knowledge, this work has not been submitted to any other University/Institute for the award of any degree or diploma.

Dr. Subrata Kumar Panda

(Supervisor)

Assistant Professor

Department of Mechanical Engineering

ACKNOWLEDGEMENT

First of all, I would like to express my ardent gratitude to my esteemed supervisor Dr. Subrata Kumar Panda, Assistant Professor (Department of Mechanical Engineering, NIT Rourkela) for his abled guidance and supervision. He has been a great inspiration for me and has helped me in every possible manner throughout this project. His undaunted cooperation and valuable advices have helped finally to complete this project successfully.

I would also like to thank Mr. Vishesh Ranjan Kar and Mr. Vijay K. Singh and, the two Ph.D Scholars from Department of Mechanical Engineering, NIT Rourkela for helping to understand the technical aspect of this project and guiding throughout the analysis part of this project by virtue of their vast experience to work with ANSYS software.

Finally, I would also like to appreciate Mr. Swayam Bikash Mishra, PhD, Department of Mechanical Engineering, NIT Rourkela for his kind support in helping me to gather all the requisite knowledge related to genetic algorithm that provided me a thorough insight into this project.

Pradosh Pritam Dash

(Roll No.: 111ME0292)

Dept. of Mechanical Engineering

NIT ROURKELA

TABLE OF CONTENTS

Abstract

The advent of microfabrication has given a great impetus to MEMS inertial sensors particularly MEMS automobile sensors. In developing Microsystem technology, FEA has been acknowledged as the most cost and time effective alternative to building a prototype for simulation. Present work focuses on developing mathematical model in order to formulate a design procedure to determine the influence of geometric attributes of a four and an eight beam cross bridged accelerometer for automotive applications pertaining to lower inertial loads (± 2g). The configuration is so chosen to minimize cross-axis sensitivity and temperature variation. The proposed mathematical model takes both mechanical and electrical aspects into consideration. Both accelerometers are doped with p-type (boron diffused) silicon at two ends of its flexures. An optimization based on genetic algorithm has been carried out to determine the best possible geometric configuration while satisfying the specification of automotive inertia sensors. A solid model based on optimized dimensions has been simulated using ANSYS to determine stress, deformation, sensitivity for both configurations followed by validation with analytical results. The two configurations have been compared on the basis of output behaviour and performance parameters, and the obtained results are described in detail.

Keywords: MEMS; FEA; Piezoresistive Accelerometer; Genetic Algorithm;

LIST OF FIGURES

LIST OF TABLES

LIST OF SYMBOLS

Symbols	Units	Description
$x\ y\ z$	Meter,(m)	Cartesian coordinate system
m	Kg	Mass of the flexural beams
M	Kg	Mass of the proof mass
ρ_o	Kg/m^3	Density of silicon
h_m	m	Height of truncated pyramid shaped proof mass
l_1	m	Top side length of proof mass
l_2	m	Base side length of proof mass
k	N/m	Spring stiffness constant
E	Gpa, Mpa	Young's Modulus of Elasticity
I	m^4	Moment of Inertia of the beam
l	m	Length of flexural silicon beam
b	m	Breadth flexural silicon beam
h	m	Thickness flexural silicon beam
μ	Pa S	Dynamic viscosity
P	Pa	Gas Pressure
h_f	M	Air film thickness
ω	Hz	Excitation frequency
ω_n	Hz	Natural Frequency
c	Ns/m	Damping Coefficient
ξ	--	Damping Ratio
a	m/s^2	Applied acceleration
$A^{'}$	m	Amplitude of vibration
ω_1, ω_2	kHz	Half power point frequencies
ω_c	kHz	Bandwidth
$R, \Delta R$	Ω	Resistance and change in resistance
L	m	Length of piezoresistor
A_c	m^2	Cross-sectional area of piezoresistor
ρ_p	Ωm	Resistivity of Piezoresistor

N	None	Number of charge carriers
q	$1.6\times10^{-19}c$	Electron charge
μ_c	cm^2/Vs	carrier mobility
σ_{yt}	MPa	Yield Strength
α	$^0c^{-1}$	Coefficient of Thermal Expansion
μ_1	(m/m)	Poison's Ratio
$\rho_{ij}, \Delta\rho_{ij}$	Ωm	Resistivity
$\pi_{11}, \pi_{22},$ π_{44} π_L, π_T	Pa^{-1}	Piezoresistive coefficients
V_{out}	mV	Output Voltage of Wheatstone Bridge
V_{in}	mV	Input Voltage of Wheatstone Bridge
δ_R	--	Relative change in resistance
G	--	Gauge factor

CHAPTER 1

1.1 Introduction

Micro-electromechanical systems (MEMS) can be termed as a portfolio of technology where several physical domains (Inertia, Displacement, Pressure etc.) are combined with a mechanical function(such as deflection of beam or stress induced) which in turn is coupled to an electrical signal. MEMS are also stated Micro Systems Technology (MST) in which sensors serve the main functionality. Micro-accelerometers or accelerometer are one of the most significant types of MEMS device, which have greatest commercial application after Pressure sensors. In the field of consumer and military applications, avionics and automobiles, MEMS sensors are of paramount importance as they offer high performance along with miniaturization. Among various types of accelerometer bulk micro-machined piezoresistive accelerometer possess an advantage in terms of simplicity of manufacturing, reliability and ability to sense down to zero frequency.

The present work focuses on FEA based design and genetic optimization followed by an electrical analysis of cantilever type piezoresistive accelerometer for low g automotive applications. Piezoresistive materials are used either in the form of a thin film or wire strain gauges. As the mechanical stress applied to piezoresistor changes, their resistance also changes. Fundamentally, the proposed accelerometer senses deformation due to inertial force and converts it into a measurable electrical signal. In order to increase sensitivity by reducing structural and thermal variations, multiple piezoresistors are used with the same mass- spring system and arranged in a Wheatstone bridge circuit. Finite Element Analysis (FEA) is a reliable tool to study and simulate MEMS in estimating temperature distribution, deformation and stress. This approach enables us to extend device performance while eliminating the need for fabrication of a prototype. Until the desired specification are achieved, simulation can be continued to improve the decision parameters, thus making the process both time and cost effective. Current work also focuses on optimizing device dimensions using a genetic algorithm that is an effective search algorithm based on Darwin's principle of natural selection. Research shows the advantages of genetic algorithms are intriguing and produce stunning results where traditional optimization approaches fail miserably. FEA in combination with Genetic Algorithm provides a complete and effective design procedure for accelerometer design, which is rarely attempted in the field of microsystem technology to date.

1.2 Literature Review

Bernstein et al. [1] stated that MEMS technology with commercial efficacy has been successfully implemented in case of accelerometers and are the current leader in automotive applications. The pioneering development began in 1988 with its implementation in Airbag crash sensors with high resolution capable of sensing greater g inertial loads. Automotive application accounts for 89 % of accelerometer market worth which was $393 million in 2005 and subsequently$869 million in 2010 [2]. High performance to cost ratio coupled with miniaturization, low power requirement and high reliability will soon make the non-MEMS components obsolete in the near future. According to Yazdi et al. [3], every two year the performance of inertial sensors has been consistently improving by a factor of 10. Since their inception in 1970 by Stanford University researchers, inertial sensors have incorporated various functionalities that have been accomplished by tremendous advancement in the field of assembly, packaging and microfabrication. Kovacs et al. [4] showed that despite the rise of high aspect ratio methodologies of surface micromachining, bulk micromachining is the most widely used in MEMS industry as it possess a great extent of versatility in etching methods along with a superior control over surface roughness and process capability. In inertial sensors, the conversion of the mechanical motion to electric signal is carried out relying on either of the following three principles: Piezoelectricity, Piezoresistivity or Capacitance.

According to [2,3], the accelerometer based on the principle of capacitance has an advantage over the other two types as they impart high sensitivity, bandwidth, low power and high precision, but Yazdi et al. recognised that high impedance capacitive device are vulnerable to interference due to electromagnetic waves. Further, their incompetence to measure DC acceleration often results in significant inconvenience that can be totally eliminated using the piezoresistive type accelerometer. However, the later suffers from temperature sensitivity.

The design procedure of accelerometer as proposed by Yazdi et al. involves defining stiffness constant as a variable depending on the geometric parameters using mathematical model followed by optimization and simulation by commercial software packages. Such design steps were implemented by Wang et al. [5], and Yu et al. [6] presented an analytical model and verified using finite element modelling. Their model consists of four symmetric suspension flexures (cantilever) attached to seismic mass in a

cross bridged fashion. Also Yu et al. applied the same fundamental procedure to a two beam optimized structure and performed a dynamic analysis to conclude that in piezoelectric type inertial sensors, under resonance conditions i.e. when the driving frequency approaches the natural frequency of the system, the maximum normal stress and the output characteristics are adversely affected which are otherwise non-significant. This study suggests operating accelerometer at max at one-third of natural frequency. Wang et al. and Yu et al. both took the elastic property and geometric specifications as input and sensitivity and frequency as output parameters. In both of the analyses, flexural mass are considered negligible as compared to the seismic mass and vibration was considered only along a direction perpendicular to the proof mass plane. Also, the stiffness of the seismic mass was not taken into account and thus derived from flexural beams only which are assumed to be straight ones. Denishev et al. [7] proposed a design procedure for piezoresistive accelerometer based on an analytical model that considered eight beam cross bridged model. The proposed flow of design was aimed to attain a predetermined minimum detectable acceleration and bandwidth whose geometric parameters were bounded by microfabrication limitations. The damping model for the same was based on squeeze film damping. Bhalla et al. [8] performed a finite element analysis on three configurations of piezoresistive accelerometers which were designed for low cross-axis sensitivity owing to their bridge type structure in which misalignment effect was minimized keeping the width very small. The Simulation was performed on COMSOL multiphysics, and the models were found to be of high shock survivability (up to +15000g). Mukhiya et al. [9] following FEM based design and simulation compared the sensitivity of two accelerometer each having four beams in a bridged manner but with different orientation and proposed a process flow for fabrication. The study was intended for low g application in the automotive sector. Biswas et al. [10] and proceeded to design bio memes for tremor detection using piezoresistive accelerometer with a dynamic range of ($\pm$) 2g considering Wheatstone bridge configuration for electrical analysis with low cross-axis sensitivity. Hrairi et al. [12] proceeded towards validating analytical results with FEM-based simulation followed by thermal analysis Agarwal et al. [14] and Baig et al. [15] both modelled the MEMS accelerometer mathematically and then determined the required geometry using shape optimization.

CHAPTER 2

2.1 Working Principle of Accelerometer

Fundamentally, any elastic structure can be modelled as a mass-spring-damper system even at the microscopic level. The vibration of a cantilever type substrate is an ideal example in this regard where there may be a seismic mass present, or it may be due to self-weight. Here flexural rigidity can be perceived as the resistance of the spring to vibration. Also, the presence of air or any other working medium causes damping. Hence, figure 1 can be taken into consideration to explain the working principle of an accelerometer. It consists of a proof mass (M), suspended by a spring (stiffness k) which in turn attached to a casing. There is also a dashpot for producing desirable damping that is parallel to the spring and have a damping coefficient (c). At the microscopic level, working medium (may be air) offers significant resistance to vibration that stabilizes the system after sudden acceleration. Acceleration of the casing will cause an inertial force to act on the system (proof mass) which will have a deflection of x.

The measurement of acceleration and subsequent deflection relies on Newton's 2nd law of motion. The equation of motion can be derived equating inertia force to the summation of the remaining real forces on the proof mass. This constitutes a second-order system of classical mechanics. According to the figure 1 for static equilibrium in the y direction,

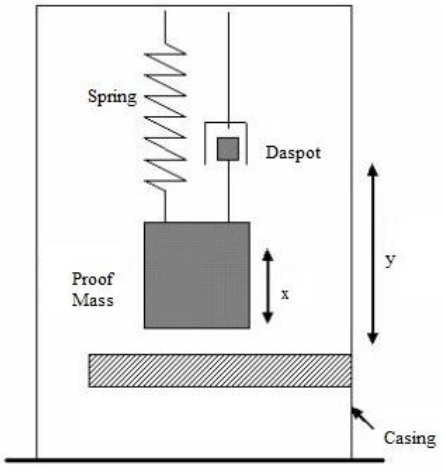

Figure 1 Lumped Model of a Piezoresistive Accelerometer

Applied force- Damping Force- Spring Force= Inertia Force

(or) $m\frac{\partial^2 x}{\partial t^2} + c\frac{\partial x}{\partial t} + kx = ma$ (1)

Where,

m= mass of the seismic mass, c=damping coefficient

k=stiffness of the spring, x=displacement of seismic mass relative to the casing

a= acceleration of the casing

This is second order linear differential equation with constant coefficients.

The general solution is of the form:

$x = x_c + x_p$

Where, x_c = complementary solution and x_p = particular solution

x_c is the solution of the homogeneous equation (1)

$$m\frac{\partial^2 x}{\partial t^2} + c\frac{\partial x}{\partial t} + kx = 0 \quad (2)$$

Assuming a solution of the form $x = e^{pt}$ and substituting,

$e^{pt}(\mathrm{mp}^2 + \mathrm{cp} + \mathrm{k}) = 0$

On solving further,

$$p = \frac{-c/m \pm \sqrt{(\mathrm{c}/\mathrm{m})^2 - k/m}}{2}$$

Substituting, natural frequency, $\omega_n = \sqrt{\frac{k}{m}}$

Critical damping coefficient, $c_c = 2m\omega_n$

And Damping Ratio, $\zeta = c/c_c$

Hence complementary solution, $x_c = C_1 e^{(-\zeta \pm \sqrt{\zeta^2 - 1})\omega \mathrm{t}}$ (3)

For underdamped condition above equation modifies to

$x_c = C_1 e^{-\zeta\omega \mathrm{t}} \cos(\sqrt{1-\zeta^2}\,\omega_n t) \pm \sin(\sqrt{1-\zeta^2}\,\omega_n t)$

Or, $x_c = C_1 e^{-\zeta\omega \mathrm{t}} \cos(\sqrt{1-\zeta^2}\,\omega_n t + \phi)$ (4)

It is apparent that with time x_c vanishes, letting the total response be equal to the steady state response (particular solution).

The particular solution can be obtained considering the vector diagram of four forces such as Inertia, spring, Harmonic and damping forces.

$$F^2 = (\mathrm{kA} - \mathrm{m}\omega^2 \mathrm{A})^2 + (\mathrm{c}\omega \mathrm{A})^2$$

Where F=ma and A= amplitude of vibration

Assuming acceleration a to be sinusoidal

$$a = \omega^2 A' \sin \omega \mathrm{t}$$

On further simplification,

$$\frac{A}{A'} = \frac{(\omega/\omega_n)^2}{\sqrt{\left[1-(\omega/\omega_n)^2\right]^2 + \left[(2\zeta\omega/\omega_n)^2\right]}} \qquad (5)$$

Usually, Accelerometers are devices of high natural frequency, i.e. $\omega \ll \omega_n \Rightarrow \frac{\omega}{\omega_n} \to 0$

so, from equation (5)

$$\frac{A}{A'} = \left(\frac{\omega}{\omega_n}\right)^2 = \frac{Accelration_{casing}}{\omega^2_n} \qquad (6)$$

It is clear from the above equation that the sensitivity of the measurement is inversely proportional to ω_n^2. Thus for high sensitivity ω_n has to be small which suggests large proof mass. Contrarily, large ω_n adversely affect the bandwidth. Hence, it is always a trade-off between bandwidth and sensitivity.

2.2 Material Selection

Silicon is particularly associated with Microsystems design as it is strongly desirable for inertial sensors with its greater flexibility in design and fabrication. Single crystal silicon shows elasticity up to fracture point, although it is lighter than even Aluminium. Its elastic modulus and melting temperature are comparable to that of stainless steel yet possess a thermal expansion coefficient eight times smaller than the later. Specifically, silicon is mechanically stable and hence signal transduction elements such as p-type or n-type piezoresistor can be integrated with its substrate. It offers no mechanical hysteresis that makes it ideal for sensors and actuators fabrication [12].

In the present work for both Finite Element Analysis and Analytical hand calculations, the silicon is approximated as an isotropic material with the properties given in Table 1. The value of young's modulus (1.69E+11) closely approximates the material properties as the orientation of the proof mass of the accelerometer is <110> after manufacturing.

Table 1 Material Properties of Silicon <110>

Isotropic Material Properties	**Symbol**	**Unit**	**Value for Silicon<110>**
Density	ρ_0	Kg / m^3	2300
Young's Modulus	E	GPa	169
Yield Strength	σ_{yt}	GPa	7
Coefficient of Thermal Expansion	α	$^oC^{-1}$	2.3
Poison's Ratio	μ_1		0.28

CHAPTER 3

3. Mathematical Modelling

3.1 Mechanical Aspect

The piezoresistive accelerometer has a proof mass at the centre, and two configuration having four and eight flexural silicon beams in a cross bridged structure are considered for modelling. The two extremities of each flexure are doped with piezoresistors of p-type single crystal silicon <110> to sense the maximum stress and design accelerometer accordingly to measure deflection where it is dominant [10]. The design procedure involves the determination of certain parameters that are proof mass side length (l_1), height (h_m) and dimensions of flexures ($l \times b \times h$) in two different configurations.

3.1.1 Silicon proof mass:

During bulk micro-machining anisotropic etching makes the proof mass shape hexagonal. Thus, the proof mass is assumed to be of truncated square pyramid shape. Its mass can be obtained by

$$m = \iiint_v \rho dxdydz = \frac{\rho h_m (l_1^2 - l_1 l_2 + l_2^2)}{3(l_1 - l_2)} \quad (7)$$

Where, Density, ρ = 2300 Kg/m^3, l_1 =top side length, l_2 =base side length

h_m =height of the pyramid. Height of the pyramid is taken $525 \mu m$

Where $l_2 = l_1 - h_m / \sqrt{2}$ [13]

3.1.2 Spring Constant:

It relies on material property and geometrical parameters of flexural beams.

Using the relation $k = 12EI / l^3$, where E =Young's modulus and moment of Inertia $I = bh^3 / 12$.

Thus, for each flexure, $k = Ebh^3 / l^3$ (8)

3.1.3 Damping Model

Damping is one of the major sources of energy dissipation and is highly dependent on viscosity. For moving MEMS surfaces, there are two models available: Squeeze film damping and side film damping. The former occurs when relative motion between two surfaces is perpendicular to the plane of the surfaces, and the later takes place when the two moving surfaces are parallel to each other. The present work focuses on the *Squeeze film damping model* following Reynolds gas-film equation. The prerequisite for this model is non-slip fluid flow that occurs when the film thickness, $h > h_{threshold}$. Where $h_{threshold}$ is 100 times the mean free path [14].

squeeze number, σ shows compressibility of the fluid film.

$$\sigma = \frac{12\mu b^2}{P h_f{}^2}\omega \tag{9}$$

Where, μ =dynamic viscosity, l_2 = base side length of proof mass, P =Gas pressure

h_f =Fluid film thickness, ω = Excitation Frequency

The damping coefficient for squeeze film damping is given by

$$c = \frac{l^2{}_2 \beta P}{\omega h_f}\frac{64\sigma}{\pi^6}\left(\frac{1+\frac{1}{\beta^2}}{\left[1+\frac{1}{\beta^2}\right]^2+\frac{\sigma^2}{\pi^4}}\right) \tag{10}$$

Where, β is the ratio of Length to breadth and 1 for square cross section

3.1.4 Natural Frequency

In reality, a micro system is a continuous complex geometry and possesses infinite mode for resonance to occur. Inherent natural frequencies of the structure cause this. To avoid catastrophic consequences of resonant vibrations natural frequency of the system is made as high as possible. Natural frequency (ω_n) is given by

$$\omega_n = \sqrt{k/m}$$

Substituting k and m values,

$$\omega_n = \sqrt{24Ebh^3/(l^2{}_1 - l_1 l_2 + l^2{}_2)\rho \mathrm{h}_m l^3} \tag{11}$$

3.1.5 Damping Ratio:

It is defined as the ration of damping coefficient to the critical damping coefficient and depends on the proof mass and spring constant.

$$\xi = \frac{c}{2\sqrt{mk}} \tag{12}$$

3.1.6 Minimum Measurable Spring Deflection:

The applied acceleration is sinusoidal, $a = \omega^2 A' \sin \omega t$ .If the acceleration is made constant, the net compression of spring varies directly with applied acceleration. Let us assume minimum measurable spring deflection $\omega_c = \left(2\zeta\sqrt{1-\zeta^2}\right)\omega^2{}_n$, where $\varepsilon_{\min}$ is minimum measurable strain of the flexural beams [13]

3.1.7 Bandwidth:

Referring to equation (3)

Magnification factor, $\frac{A(\omega)}{A(0)} = \frac{1}{\sqrt{\left[1-(\omega/\omega_n)^2\right]^2 + \left[(2\zeta\omega/\omega_n)^2\right]}}$ (13)

At resonance $\omega = \omega_n$

Thus, Quality factor $R = \frac{A(\omega_n)}{A(0)} = \frac{1}{2\xi}$

Taking two half-power points on both sides of resonance, Equation 13 becomes

$$\frac{A(\omega)}{A(0)} = \frac{R}{\sqrt{2}}$$

Solving the above equation for $(\omega/\omega_n)^2 = (1-2\zeta) \pm 2\zeta\sqrt{1-\zeta^2}$

Hence, Bandwidth $\omega_c = \frac{\omega_2 - \omega_1}{\omega_n} = \left(2\zeta\sqrt{1-\zeta^2}\right)\omega^2{}_n$ (14)

3.2 Electrical Aspect

3.2.1 Piezoresistivity

Piezoresistivity is extensively exploited in MEMS Inertial Sensors. Silicon based poezoresistors facilitates strain transmission without creep, hence possess a higher compatibility with MEMS and Microsystems. Also, the fabrication process allows implementation of Wheatstone bridge circuits with proper matching resistors [14]. The change in resistance is $R = \rho L / A_c$ where ρ, L and A_c are resistivity, length and cross sectional area respectively. Hence, there exists a linear relationship between strain and resistance that is governing the principle of piezoresistive sensing.

In general resistivity is expressed by

$$\rho = \frac{1}{qN\mu_c} \tag{15}$$

Where, q =Electron charge($1.6\times10^{-19} c$)

N =Number of charge carriers

μ_c =carrier mobility (cm^2 / Vs)

As a single layer doped silicon is highly anisotropic, the relative orientation of crystallographic planes dictates its piezoresistivity. The resistivity is a function of direction dependent stress. It can be expressed as the sum of resistivity in an unstressed crystal and the resistivity change due to the application of stress.

$$\begin{Bmatrix} \rho_{xx} \\ \rho_{yy} \\ \rho_{zz} \\ \rho_{xy} \\ \rho_{yz} \\ \rho_{zx} \end{Bmatrix} = \begin{Bmatrix} \rho \\ \rho \\ \rho \\ 0 \\ 0 \\ 0 \end{Bmatrix} + \begin{Bmatrix} \Delta\rho_{xx} \\ \Delta\rho_{yy} \\ \Delta\rho_{zz} \\ \Delta\rho_{xy} \\ \Delta\rho_{yz} \\ \Delta\rho_{zx} \end{Bmatrix} \tag{16}$$

By incorporating piezoelectric coefficients (π_{ij}), the resistivity change ($\Delta\rho_{ij}$) can be quantified $\frac{1}{\rho}\{\Delta\rho\} = [\pi]\{\sigma\}$. For a cubic lattice, because of symmetry, π reduces to three components such as $\pi_{11}, \pi_{12}, \pi_{44}$. To define piezoresistivity for any random orientation we

need to define longitudinal π_L and transverse (π_T) piezoresistive coefficients, which can be obtained by transforming the axes from an orientation where the piezoelectric coefficients are known.

Finally, the resistance change can be expressed as

$$\frac{\Delta\rho}{\rho} = \frac{\Delta R}{R} = \pi_L \sigma_L + \pi_T \sigma_T . \quad (17)$$

Where σ_L and σ_T represents longitudinal and transverse stress components respectively.

Piezoresistive coefficients π_{11}, π_{12} and π_{44} decrease with an increase in temperature and doping concentrations. If the stress and electric field are applied in the same direction, the piezoresistirs is said to be longitudinally stressed. For such a situation $\pi_L = \frac{1}{2}(\pi_{11} + \pi_{12} + \pi_{44})$. Piezoresistive coefficient for the <110> orientation of a single crystal silicon is expressed as $\pi_L = 0.5(\pi_{11} + \pi_{12} + \pi_{44}) \approx 0.5(\pi_{44})$ (18)

The value of π_L at room temperature is 69.05×10^{-11} Pa^{-1} [15].

3.2.2 Piezoresistor Positioning:

As sensing uses piezoresistive principle, it is easy to fabricate and integrate with electronic circuits. Boron diffused resistors were placed at the positions where stress is maximum for maximum utilization of piezoresistive characteristic of silicon. In the present work, two different models of piezoresistors are conceived using (1) four beam flexure (figure 2) and (2) eight beam cross bridged flexure configurations. Each flexure spans from the frame end to the proof mass end. Hence, for each flexure, there are two resistors diffused at the junction with a proof mass (R_m) and that with frame (R_f). When the structure is under inertial loading the stress on these two ends are opposite in nature [8].

Piezoresistors are placed longitudinally on the beam so that their resistance decreases under compressive force and increases under tensile forces. This effect is summarized as follows with reference to the circuit diagram for the two configurations.

Table 2 Nature of Stress induced as a result of inertia loading along prime axis of motion

Configu-ration	R_{m1}	R_{f1}	R_{m2}	R_{f2}	R_{m3}	R_{f3}	R_{m4}	R_{f4}	R_{m5}	R_{f5}	R_{m6}	R_{f6}	R_{m7}	R_{f7}	R_{m8}	R_{f8}
Four Beam	T	C	T	C	T	C	T	C	(Not Applicable)							
Eight Beam	T	C	T	C	T	C	T	C	T	C	T	C	T	C	T	C
(T)= Tensile stress, (C)= Compressive stress																

3.2.3 Wheatstone bridge description:

For piezoresistive devices, there is no requirement of circuitry on the chip. Instead half or full Wheatstone bridge can be implemented for signal detection with high sensitivity and first-order temperature compensation [14]. Two piezoresistor are doped on the proof mass end and frame end of each flexure. It can be observed that stress on the two ends is of opposite sign.

Hence in the proposed set up resistance of the piezoresistor near the proof mass increases under tensile forces and that of the piezoresistors at the frame end decrease[9].For the first configuration, all eight resistor form a fully active Wheatstone bridge as shown in the figure s2. Similarly for the second configuration (8 flexures in a bridge structure) a total of 16 resistors form a wheat stone bridge as shown in figure 3.

For a fully active Wheatstone bridge

$$V_{out} = \delta_R V_{in}, \tag{19}$$

Where, $\delta_R = \Delta R / \mathrm{R}$

V_{out} =Output Voltage, V_{in} =Input Voltage

Change in voltage of the Wheatstone bridge is proportional to the applied acceleration. [10].Hence, sensitivity can be determined by the relative change in output voltage for the applied acceleration. Alternatively gauge factor can be used to determine the sensitivity that is the ratio of resistance change to induced strain, $G = \frac{\Delta R}{R}\frac{1}{\varepsilon}$.

(20)

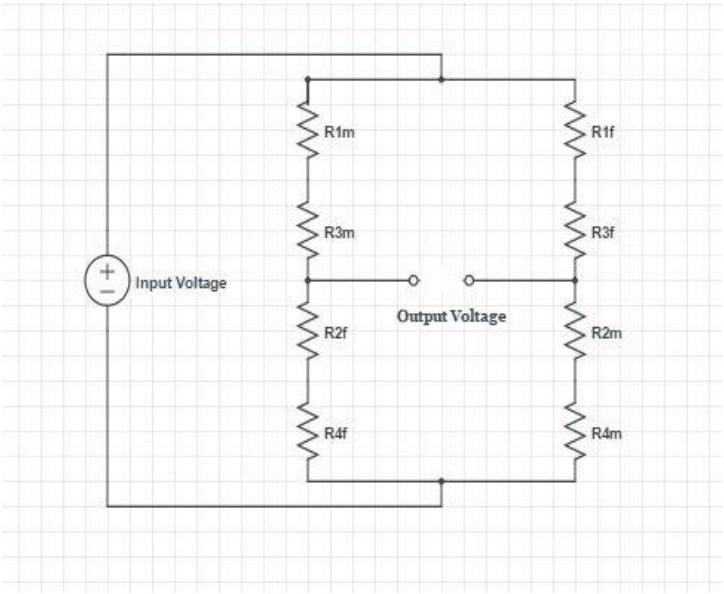

Figure 2 Wheatstone bridge configuration with piezoresistors for four beam cross bridged configuration

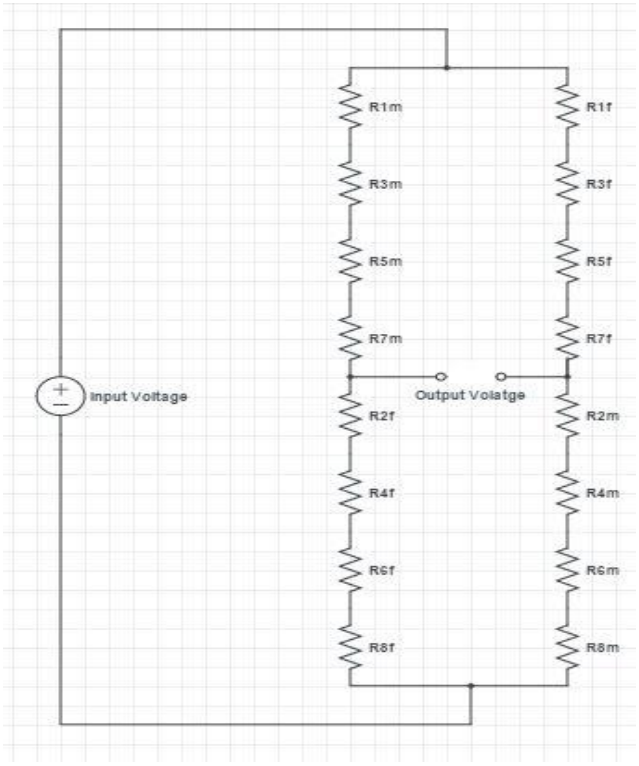

Figure 3 Wheatstone bridge configuration with piezoresistors for Eight beam cross bridged configuration

CHAPTER 4

4.1 Optimization of Geometric Parameters

Once the solution space is determined from micromachining, it can be integrated with a genetic algorithm to optimize by performing advanced adaptive searching mechanisms based on Darwin's natural selection of the fittest and genetic evolution. , the search algorithm incorporates survival of the fittest between string structures with randomized information exchange yet in a structured manner with a pioneering flair of human search. It essentially exploits the fittest traits of the parent generation to create a new artificial child string in an iterative process that gets better with each subsequent generation. Thus, it combines historical information to find new data points while matching the desired performance. In the present work, the objective is to obtain a set of geometric parameters that best fits the desired specification. The device dimensions of the accelerometer involves the following: The design procedure involves determination of certain parameters that are proof mass side length (s), height (h_m) and dimensions of flexures ($l \times b \times h$) and depth of the air film thickness(h_f). To reduce cycle time for design, the die area must be minimized. Simultaneously, attention must be given not to deteriorate the device performance. This calls for the implementation of evolutionary optimization algorithms such as Genetic Algorithm (GA) and Particle Swarm Optimization (PSO) [14]**.**

However, there is no certainty to obtain the best-desired solution, but a suitable solution with least processing time is guaranteed. In situations where classical methods are inefficient in finding a suitable solution because of the presence of local extremes, Genetic Algorithm can be successfully used to search the best possible solution. In the present work MATLAB optimization toolbox based on genetic algorithm has been used**.** It has a single objective function that must be chosen properly to make the optimization flow into right path. The wafer area is to be minimized. Wafer area consists of an area of the beams and the proof mass. With the mathematical models as input the four and eight bridge structures are optimized to achieve the targeted specifications. The performance specification applies three constraints pertaining to minimum detectable acceleration, bandwidth and damping ratio that are listed below:

Table 3 Targeted specification of accelerometer

Parameter	**Targeted Specification**
Band Width, ω_c	More than 4 kHz
Minimum detectable acceleration $a_{\min}$	Minimum 0.025g
Damping Ratio, ζ	0.6-1.1
Natural Frequency, ω_n	More than 1kHz
Sensitivity (Gauge Factor)	Minimum 100

Though using micromachining significant miniaturization is possible, there are some practical limitations to it in terms of geometric parameters of the structure to be manufactured. These limits constitute the solution space for proposed genetic algorithm. The limits as found out by [8] are as follows.

Table 4 Solution Space for Geometrical parameters due to Micromachining limitations

Parameter	**Lower Bound** $(\times 10^{-6} m)$	**Upper Bound** $(\times 10^{-6} m)$
l_1	1000	5000
l	300	600
b	100	300
h	2	10
h_f	5	40
h_m	250	525

MATLAB toolbox for Genetic optimization requires various parameters to be chosen as per the desired environment. For the present work, paretofraction, elite count and the crossover fraction were selected optimally. Time and stall limit were set at infinity by default. As it is a minimization problem, the fitness limit is chosen minus infinity. The optimization algorithm

is applied first considering the four beam bridged MEMS structure and then for eight beam cross bridge MEMS structure. The obtained results are tabulated in the following manner:

Table 5 Device parameters optimized by genetic algorithm

Parameter ($\times 10^{-6} m$)	**Accelerometer Configuration**	
	four beam	**Eight beam**
l_1	2417	2425
l	363	405
b	257	260
h	5.39	4.69
h_f	9.5	37
h_m	524	525

Using the mathematical model described earlier the expected device performance parameters were calculated and tabulated in the following. It can be seen that all the performance parameters are within the required specification and hence acceptable.

Table 6 Expected Device performance

Expected Device Performance	**Accelerometer Configuration**	
	four beam	**Eight beam**
Band Width, ω_c	9.87 kHz	9.99 kHz
Minimum detectable acceleration $a_{\min}$	0.00193g	0.00209g
Damping Ratio, ζ	0.60	0.66
Natural Frequency, ω_n	14.5 kHz	10.07kHz

4.2 3D Model Construction

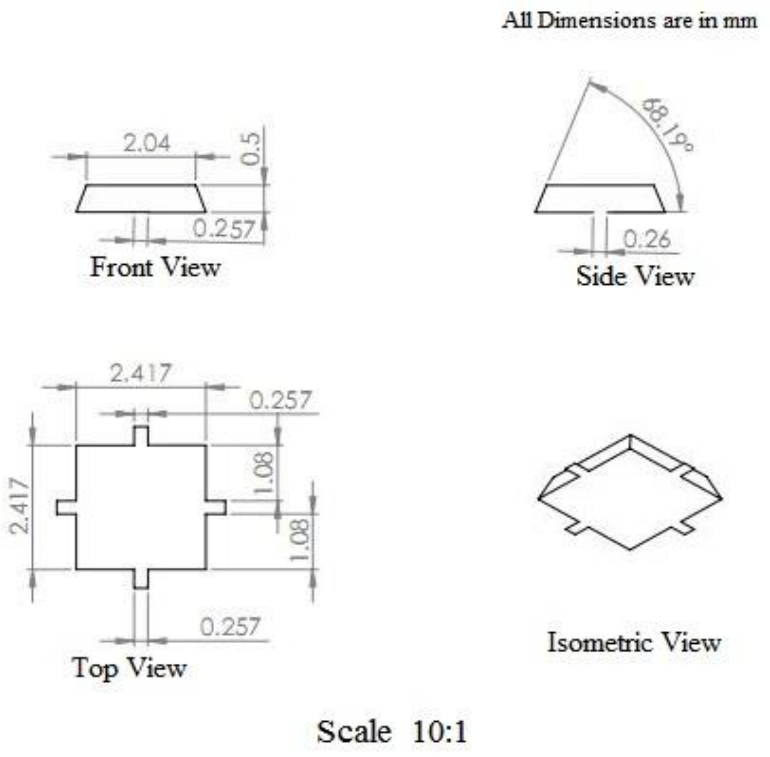

Figure 4 Solid works model of four beam cross bridged accelerometer

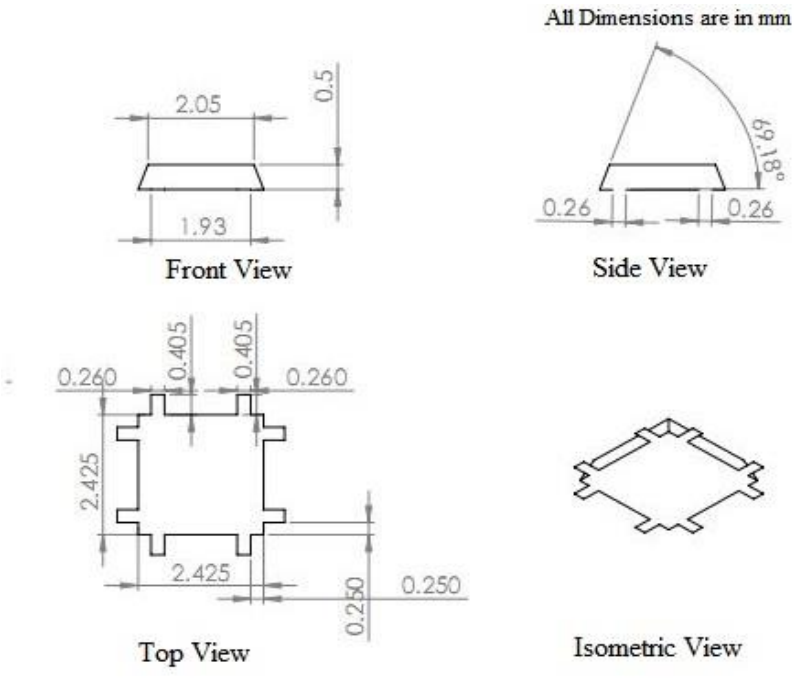

Figure 5 Solid works model of four beam cross bridged accelerometer

CHAPTER 5

5.1 Analytical Results

The geometric parameter for each configuration of the MEMS was selected as obtained from the genetic optimization. Considering the material properties for isotropic silicon from table 1, a mechanical analysis has been performed using the mathematical model derived in section 5.The inertia load in the analysis is assumed to be +g along the prime (axis perpendicular to the proof mass top surface).

The results obtain are represented in table 7 below.

Table 7 Results from mechanical analysis of piezoresistive accelerometer

Mechanical Parameter	**Unit**	**Formula**	**Configuration of Accelerometer**	
			Four Beam	**Eight Beam**
Mass of Proof mass(M)	Kg	Volume × Density	6.9912×10^{-6}	6.058×10^{-6}
Mass of beam (m)	Kg	Volume × Density	1.156×10^{-9}	1.135×10^{-9}
Moment of Inertia(I)	m^4	(Beam Width × Beam height^3)/12	3.353×10^{-21}	2.2351×10^{-21}
Inertial Load	m/s^2	Acceleration	9.81	9.81
Maximum force on each proof mass	N	Mass of Proof mass(M) × Acceleration	6.86×10^{-5}	5.943×10^{-5}
Maximum force on each flexure	N	(Maximum force on each proof mass)/ number of beams	1.715×10^{-5}	0.743×10^{-5}
Deflection along prime(transverse)axis	m	(Maximum force on each flexure × Beam length^3)/12EI	0.904×10^{-7}	0.82×10^{-7}
Longitudinal Bending stress	MPa	(Bending moment × distance from neutral axis)/ I	2.16	1.57
Stiffness constant	N/m	Force on beam/ Deflection	129.9	91.96

5.2 Finite Element Modelling

The 3D modelling for the piezoresistive MEMS accelerometer is carried out using Solid Works for both four beam and eight beam configuration. The IGES model thus obtained is simulated using ANSYS workbench 2015. The material property has been selected from table 1 considering the proof mass orientation <110>.Meshing has been done using 10 node tetrahedral element as shown in figure 6 and 7**.** As the analytical model is based on a second-order partial differential equation, the mesh density plays an important role in obtaining an accurate discrete solution. Multiple mesh models of different density were chosen and consequently an optimized density is determined in each of the two proposed configurations. The total no of mess elements and nodes used in four beam cross bridged and eight beam cross bridged accelerometer are shown in table 8. A static structural analysis is then performed. The frame end centres are fixed choosing proper boundary conditions. The simulations are carried out applying +g inertial load along the prime axis of oscillation for normal stress distribution along longitudinal direction of beam, Von-misses equivalent stress distribution, directional deformation along prime axis and the total deformation which are discussed at length in the following sections.

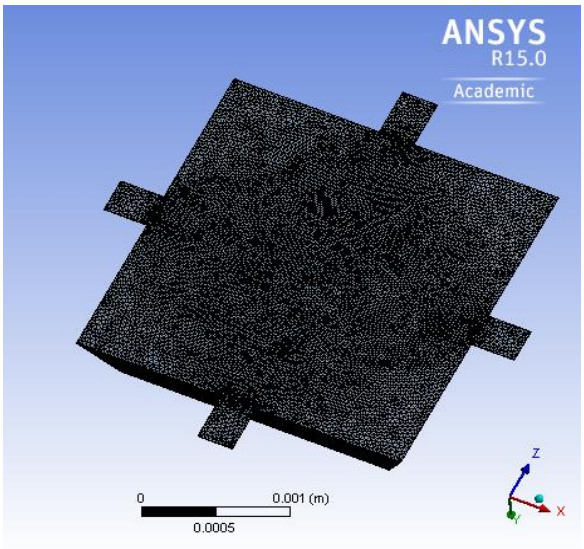

Figure 6 Meshed model for Four Beam Cross Bridged Accelerometer

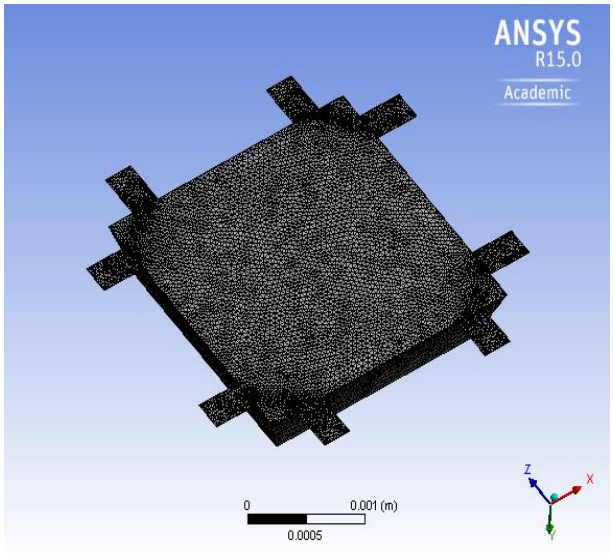

Figure 7 Meshed model for Four Beam Cross Bridged Accelerometer

Table 8 Mesh Parameters of Static structural analysis

		Nodes	**Elements**
Accelerometer Configuration	Four Beam	408847	282509
	Eight Beam	357024	244315

5.3 Results and discussions

The normal and equivalent stress distribution along the longitudinal direction shows that for both configurations maximum magnitude of the stress is found at two ends (proof mass end and frame end) which are opposite in nature. These are the precise position which are proposed to be doped by p-type (boron diffused) silicon to impart piezoresistivity. The variation of beam bending stress over the beam length has been determined and plotted in figure 7. The maximum normal stress is found to be 1.6MPa and 2.4 MPa for eight and four beam configurations respectively. From analytical hand calculations, these values were obtained as 1.57 MPa and 2.16 MPa, thus leading to an error of 1.00% and 1.87% respectively. Also, it can be observed that the four beam configuration is more stressed than the eight beam configuration. From the von-mises stress distribution, the maximum equivalent stress is 1.31 MPa and 1.89 MPa for four and eight beam configuration respectively. This gives us a quite clear idea about the maximum inertia load the device can withstand before failure. As the yield strength of single crystalline silicon is 7 GPa, an inertial load of +g is much below the maximum value. The proposed accelerometer is designed to measure transverse acceleration. Hence, deflection analysis along the same is also performed. The directional deformation along the prime axis of motion (transverse axis) is determined over the entire length of the beam is determined. As the frame, end is fixed the obtained displacement is zero there, and it is maximum at the proof mass end. The variation is plotted as shown in figure 8. The analytical values of directional deformation are also compared with FEA values which showed an error of 1.3 % and -1.1 % for four beam and eight beam configurations respectively. Comparative results for both displacement and stress simulation results between analytical and FEA values are tabulated in table 9. A sensitivity analysis is also performed for both configurations using the (17) and (20). The sensitivity is expressed in terms of output voltage per unit g-force and Gauge Factor of the Wheatstone bridge. The results obtained are tabulated in table 10. Thereafter the accelerometer structures are subjected up to 5g inertial load, and the variation of relative resistance change is plotted in figure 9.

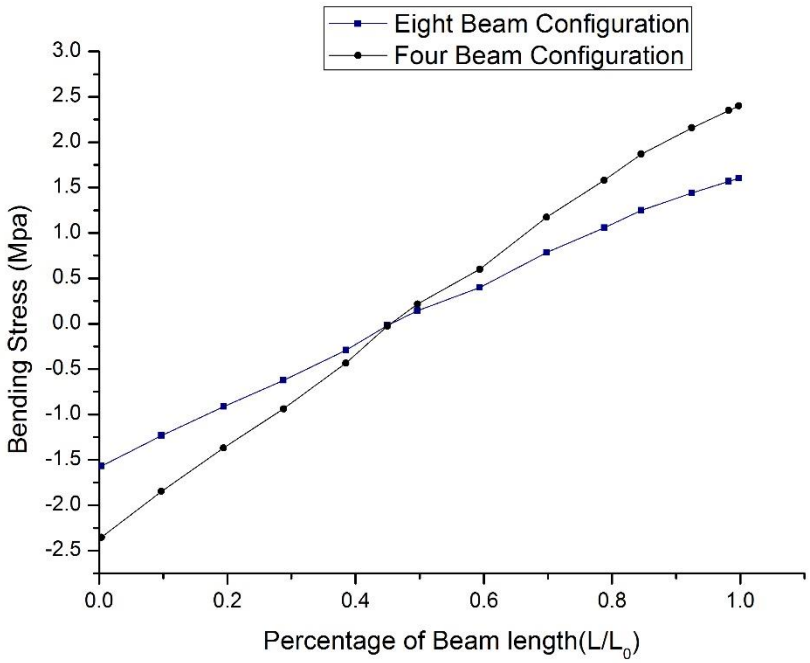

Figure 8 Variation of longitudinal bending stress over the beam length

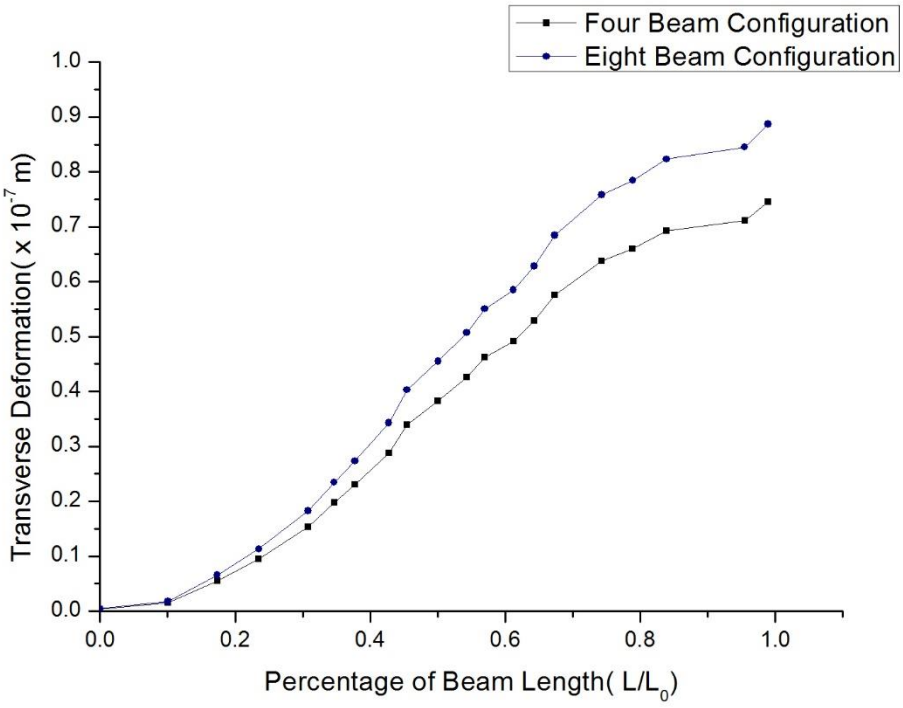

Figure 9 Variation of transverse deformation over the beam length

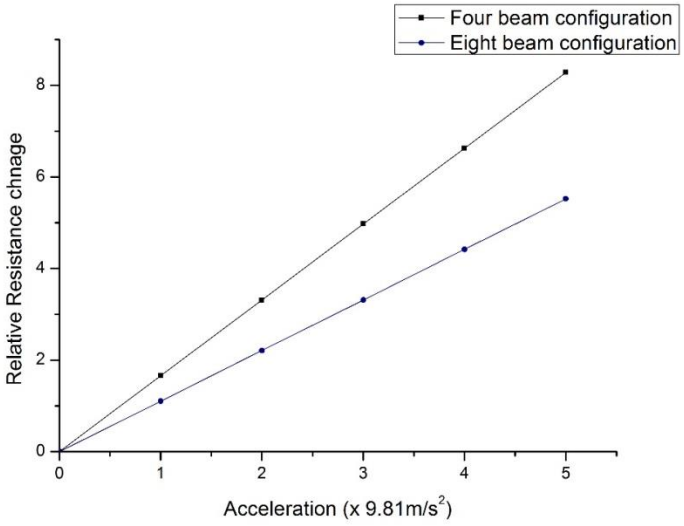

Figure 10 Variation of relative resistance of Wheatstone bridge with acceleration

Table 9 Comparative study of analytical and FEA results for static structural analysis

	Accelerometer Configuration					
	Four Beam Type			Eight Beam Type		
	Analytical	FEA	Error (%)	Analytical	FEA	Error (%)
Bending Stress (longitudinal) (MPa)	2.16	2.4	1	1.57	1.6	1.8
Directional Deformation ($\times 10^{-7}$ m)	0.724	0.74	1.3	0.89	0.88	-1.1

Table 10 Sensitivity analysis results for four beam and 8 beam configuration

	Accelerometer Configuration	
	Four Beam Type	Eight Beam Type
Sensitivity(S) $\Delta R / (R\Delta g)$ (mV/g)	1.6572	1.1048
Gauge Factor(G)	144.44	149

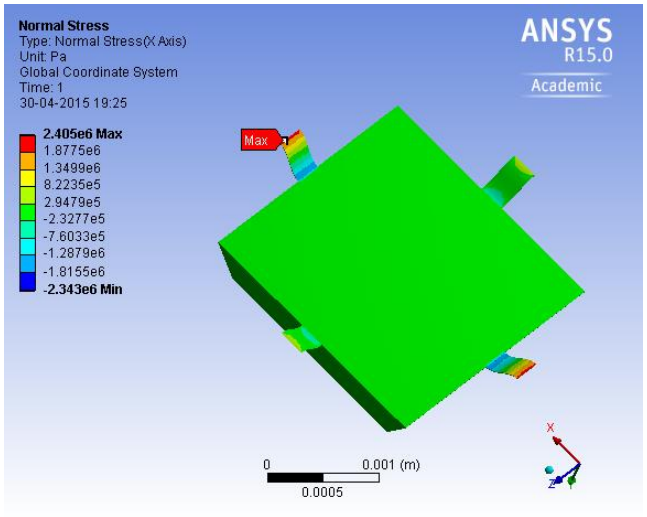

Figure 11 Longitudinal bending stress for four beam accelerometer configuration with an inertial load of +g

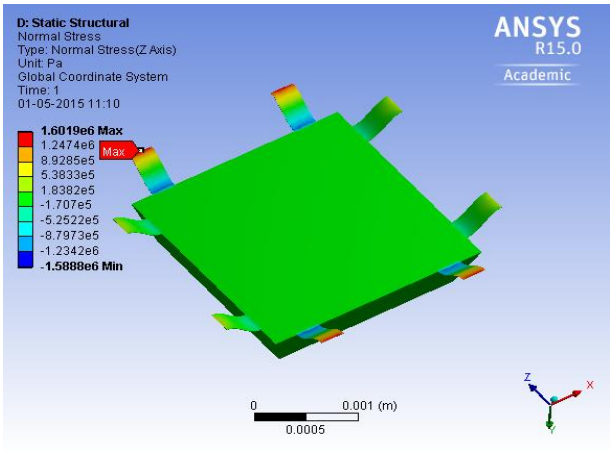

Figure 12 Longitudinal bending stress for eight beam accelerometer configuration with an inertial load of +g

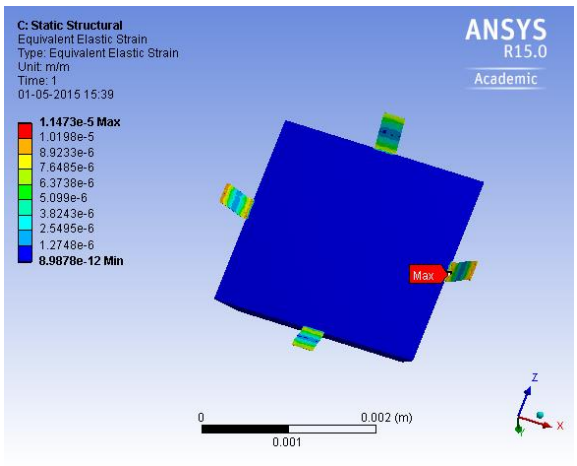

Figure 13 Transverse strain in beams for four beam accelerometer configuration with an inertial load of +g

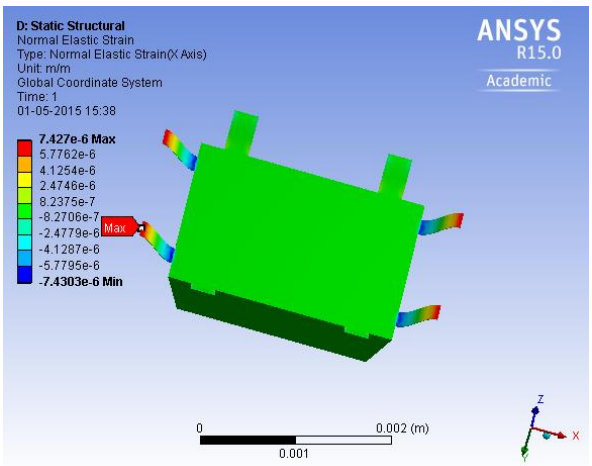

Figure 14 Transverse strain in beams for eight beam accelerometer configuration with an inertial load of +g

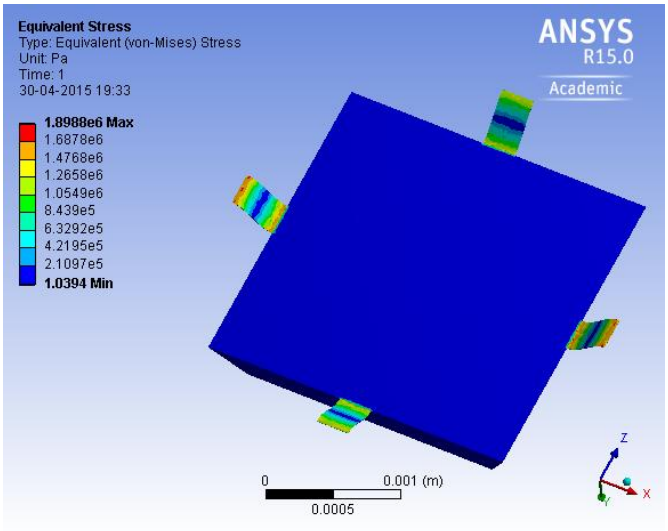

Figure 15 Equivalent(Von-mises))stress for four beam accelerometer configuration with an inertial load of +g

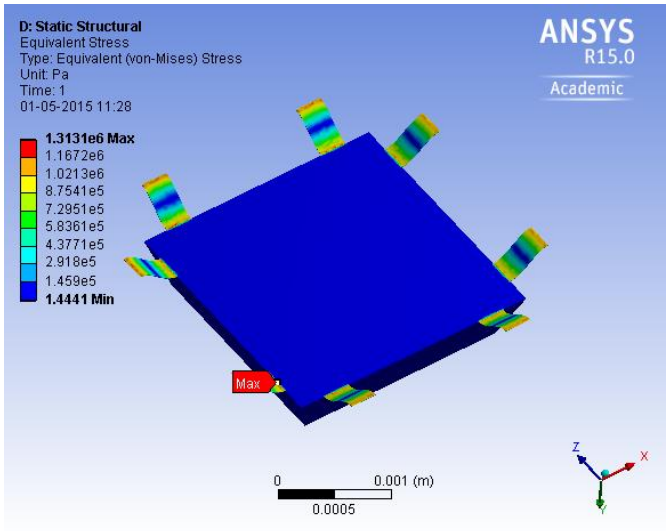

Figure 16 Equivalent(Von-mises))stress for eight beam accelerometer configuration with an inertial load of +g

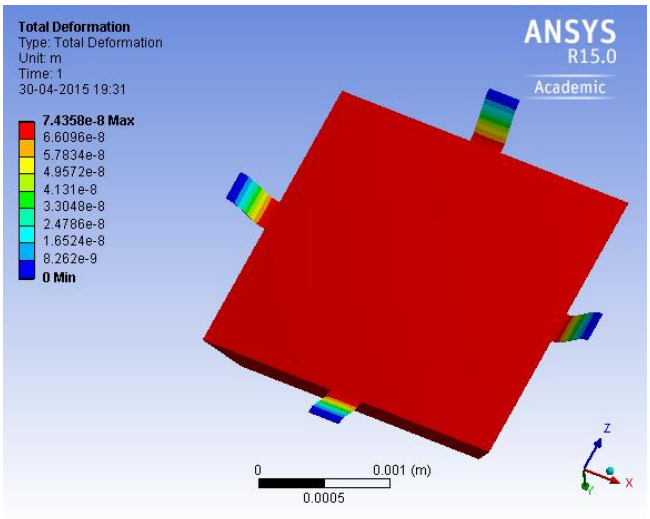

Figure 17 Transverse deflection for four beam accelerometer configuration with an inertial load of +g

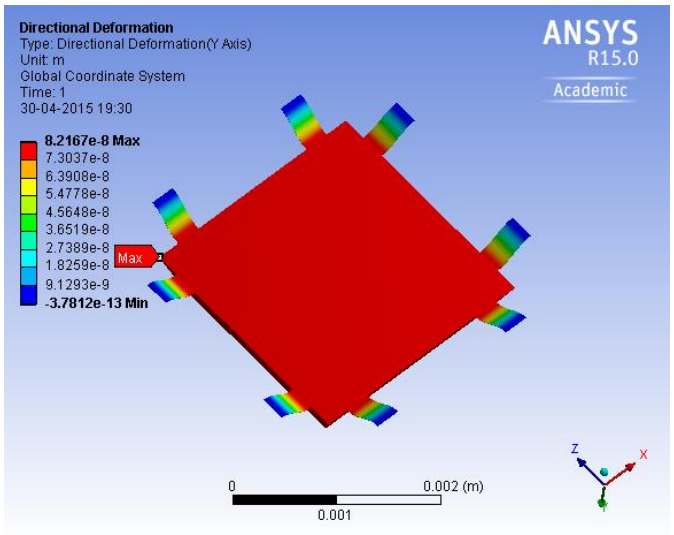

Figure 18 Transverse deflection for Eight beam accelerometer configuration with an inertial load of +g

CHAPTER 6

6.1 Conclusions

Piezoresistive MEMS accelerometer for automotive applications (low g) has been the focus of this research work.The efficacy of genetic algorithm for optimizing device dimensions and subsequent Finite Element based simulation have been explored. Implementation of neurogenetic search algorithm has reduced computational effort by searching through the nonlinear objective function and constraints to match the desired specification certainly; it is much sought after in automotive MEMS industry. Use of ANSYS for behaviour simulation of MEMS devices offers a great deal of efficiencies in design review and evaluation along with comparison with analytical results, thereby reducing design cycle time.

After an intensive study of available accelerometer structures, two configuration having four and eight beams respectively have been compared with every desired behaviour of an automotive MEMS accelerometer. Though, piezoresistors are vulnerable to temperature fluctuations and cross-axis sensitivity the present model takes care of both using a cross bridged structure. Based on the working principle of a spring-mass dashpot system a mathematical model has been developed considering both mechanical and electrical aspects and is incorporated in the genetic algorithm to determine the geometric parameters. The CAD model based on this geometric specification has been simulated for maximum stress deformation and sensitivity, and the results have been found to be in good agreement with analytical results. Thus it, shows the efficiency of the design procedure. Of the two structure considered for modelling, four beam structure is found to be more effective in terms of matching the desired specification such as bandwidth, minimum detectable acceleration and damping ratio than the eight beam counterpart. For different inertia loads on the two proposed accelerometer configurations, which reveals that the four beam structure has high sensitivity all the time. However, the later has an advantage over the former in terms of low cross-axis sensitivity.

Overall, a completely exhaustive design procedure has been proposed to meet the standard characteristics of the accelerometer with less computational cost and time.

6.2 Future Scope of the work:

In a sense, I have attempted to scratch only the surface of the FEM-based modelling for Automotive MEMS. The following aspects which are not covered by the research work and can aptly be explored.

- A squeeze film damping model has been integrated with the model, but a thorough CFD analysis is required to understand the damping behaviour of air in the encapsulation.
- Present ANSYS model simulates the mechanical behaviour and then the results approximates the piezoresistivity using analytical model. In future, a completely integrated module such as COMSOL can be implemented.
- A noise analysis can be performed to study the thermal motion and its effect on Total Noise equivalent Acceleration (TNEA) can be carried out in future.
- A frequency analysis of the three basic modes of vibration will be helpful in ascertaining the effect of geometrical parameters on natural frequency.

References

[1] Bernstein Jonathan, *An Overview of MEMS Inertial Sensing TechnologyFebruary* 1, 2003, Corning-IntelliSense Corp. Corning-IntelliSense Corp. sensor mag. pp. 45-55.

[2] Maluf N, *Introduction to micro electro mechanical systems engineering*, Boston Artech house,2000

[3] Yazdi N et al. Micromachined inertial sensors, Proc. IEEE 86: 1640–1659

[4] G. Kovacs, N. Malouf, K. E. Petersen, "Bulk micromachining of silicon," Proceedings of the IEEE, vol. 86, no. 8, pp. 1536-1551, 1998.

[5] Wang QM, Yang Z, Sensors and Actuators A: Physical. 2004; vol.113, pp. 1–11

[6] u J-C et al., Sensors and Actuators A, 2001; vol.88, 2: pp.178–186

[7] Denishev K. H, and Petrova M. R, "Accelerometer design", Proceedings of ELECTRONICS'2007, 2007, pp. 159-164.

[8] Bhalla N ,Li Sheng-Shian, Chung Danny Wen-Yaw , *Finite element analysis of mems square piezoresistive accelerometer designs with low crosstalk*, Proc. international conference on Semiconductors(CAS),2001 October, Volume 2, pp. 353-356.

[9] Mukhiya R, Adami A, Bagolini A, *FEM based design and simulation of Bulk micromachined MEMS accelerometer with Low Cross Axis sensitivity*. In proc. Seventh International Conf. on Thermal, Mechanical and Multiphysics Simulation and Experiments in Micro-Electronics and Microsystems, EuorSime, April 2006,pp-1-5

[10] Biswas S, *Design and analysis of FEM based MEMS accelerometer for detection of postural tremor in Thyrotoxicosis*, Advanced Electronic Systems (ICAES), 2013 International Conference 2013, pp.113-116

[11] Hsu Tai-Ran. *MEMS and Microsystems: Design and manufacture*, New York, McGraw-Hill Education,2002

[12] Hrairi M,Baharom B, *Design and Modelling of Silicon MEMS Accelerometer*, International Journal of Engineering Systems Modelling and Simulation, 5 (4). pp. 181-187.

[13] Allen James J., *Micro Electro Mechanical System Design*, New York, Taylor and Francis Group,2005

[14] Agarwal Vivek Design steps for bulk micro-machined single axis silicon capacitive accelerometer with optimised device dimensions, Journal of Physics: Conference Series 34 (2006), pp. 722–727

[15] Baig A, Mahmood I. *Modelling MEMS for Automotive Applications*, SAE Technical Paper 2005-01-1447, SAE World Congress and Exhibition. vol10(2005),pp. 42-71